Electrochemically-derived graphene oxide membranes with high stability and superior ionic sieving

Journal Name

COMMUNICATION

Electrochemically-derived graphene oxide membrane with high stability and superior ionic sieving

Received 00th January 20xx,
Accepted 00th January 20xx

DOI: 10.1039/x0xx00000x

www.rsc.org/

Pei Yu[a], Zhiyuan Xiong[a, b], Hualin Zhan[b], Ke Xie[b], Yu Lin Zhong[c], George P. Simon[a], and Dan Li[a, b]*

Crosslinker-free electrochemically-derived graphene oxide membranes are found to beextraordinarily stable in aqueous solutions and exhibit superior ionic sieving performance because of their unique chemical structure.

Nanofiltration membranes have wide applications in numerous fields, such as water purification, molecular separation, desalination, controlled release and so on.[1-3] Graphene oxide (GO), a graphene derivative synthesized from the chemical oxidation of graphite, is recently developed as promising two-dimensional building blocks for nanofiltration membranes.[4-6] GO membranes have laminar structure in which the oxidized sp^3 zones with carboxylic acid and hydroxyl groups act as spacer for pristine graphitic sp^2 zones to form nanoscale channel. [7-10] GO membranes thus show high water permeability because of the hydrophilic characteristics of sp^3 zones and frictionless water flow in sp^3 zones.[9, 11] Meanwhile, the tuneable nanochannels in the laminar structure can act as molecular sieves, affording GO membranes with extraordinary separation properties, including precise and ultrafast ion sieving[11-13], and high-flux and high-selectivity gas separation[7, 8]. However, GO membranes suffer from low stability in aqueous media.[14, 15] When a GO membrane is immersed in aqueous solution, the laminar structure is susceptible to swell and disintegration under the repulsive electrostatic forces caused by the negatively charged oxygen groups.[14] GO membranes have generally been considered unsuitable for use in water unless they are cross-linked with cations, macromolecules and polymers or by partial reduction.[15-20]

Electrochemical oxidation of graphite is another promising method to produce graphene oxide (EGO), which has attracted increasing interest due to potentially scalable production and more environmentally-friendly nature of the process.[21-26] Recently, various electrochemical oxidation methods have been reported to produce EGO with increased oxidation degrees, making it dispersible in water.[21, 23, 27] With the increased processability, EGO presents a promising candidate to be fabricated into hierarchical structures. However, previous studies have focused mainly on the study of electrochemical process and characterization of the produced EGO sheets at the atomic scale. EGO sheets have rarely been assembled into macroscale membranes that have a broad range of potential applications, and knowledge gaps between the structure and properties of the EGO membranes remain.

In this work, we fabricated crosslinker-free EGO membranes which was found to exhibit extraordinary stability in aqueous solution. The structural analysis showed a consistent interlayer spacing and an ordered structure within the EGO membranes after prolonged immersion in water. Ionic sieving and water permeation properties were tested, and EGO membrane showed higher ionic rejections, alongside larger water flux, than membranes comprised of chemically-derived graphene oxide (CGO). The membranes from EGO also maintained their structure and property stability during long periods of ionic sieving. The structural and chemical characterization of EGO was also undertaken to understand the relationship between these properties.

EGO was prepared via electrochemical oxidation of graphite foil by using a Tee-cell setup, similar to a previous report.[22] The electrochemical process involves three main stages: conversion of graphite into a graphite intercalation compound (GIC), oxidation of GIC into graphite oxide and finally, oxygen evolution at the Pt electrode. In this study, graphite was oxidized until the third stage was reached, by which complete electro-oxidation to EGO would have been achieved.

[a] *Department of Materials Science and Engineering, Monash University, Clayton, Victoria, Australia*
[b] *Department of Chemical Engineering, University of Melbourne, Parkville, Victoria, Australia*
[c] *Centre for Clean Environment and Energy, School of Environment and Science, Gold Coast Campus, Griffith University, Gold Coast, Queensland 4222,*

†Electronic Supplementary Information (ESI) available: [details of any supplementary information available should be included here]. See DOI: 10.1039/x0xx00000x

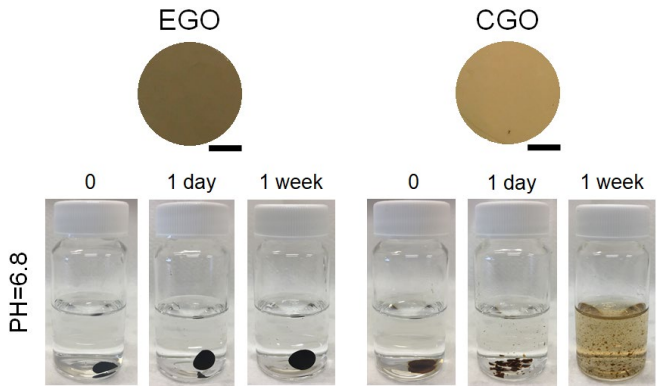

Figure 1 Top: EGO and CGO membranes with the same areal mass of 0.1 mg/cm2 (Scale bar: 4 mm). Bottom: stability of EGO and CGO membrane immersed in neutral water (pH=6.8).

Subsequently, the highly oxidized EGO was washed and exfoliated into monolayer nanosheets in water to form stable dispersion with concentration up to 4 mg mL^{-1}. (see detailed synthesis and characterizations of EGO in **ESI-1**, **ESI-2** and **Figure S1-S5**). EGO and CGO membranes were fabricated via vacuum filtration of the EGO or CGO dispersion. Because polycarbonate filter membranes were used as substrates, EGO and CGO membranes are considered to be crosslinker-free without any addition of external ions to strengthen the membranes forces.[15] After drying, free-standing EGO and CGO membranes with good consistency and uniformity were obtained (**Figure 1**). The only distinct difference in appearance of the two membranes is that when the mass loading of the membrane is low (0.1 mg/cm^2), the CGO membrane is more yellowish, whilst the EGO membrane has a brown colour.

We then studied the stability of EGO and CGO membranes in acidic (pH=1.5), neutral (pH=6.8) and basic (pH=10.5) aqueous solutions. **Figure 1** displays the photographs of EGO and CGO membranes after immersion in neutral aqueous solution (pH=6.8). Similar to the previous reports,[15] CGO membranes showed poor integrity in aqueous solutions, and cleaved into pieces after one day of immersion due to the repulsion between the negatively charged sheets (at neutral pH). After one week, CGO membranes were almost completely disintegrated into the aqueous solution. In comparison, EGO membranes were structurally very stable for at least one week of testing. In acid and base solutions (**Figure S6**), EGO membranes also retained their integrity without any evident cracking after one-week of immersion.

The structural changes of EGO and CGO membrane in water were studied via X-ray diffraction (XRD). As shown in **Figure 2a and 2b**, both EGO and CGO membranes showed an initial peak at around 12° in the dry state, corresponding to an interlayer distance of about 0.74 nm. When EGO and CGO membranes were immersed in water, their XRD peaks shifted to a smaller 2θ value, indicating an increase in interlayer distance. The changes in the interlayer distances of both the GO membranes with respect to their immersion time are shown in **Figure 2c**. Both CGO and EGO membranes showed an abrupt increase of interlayer distance after immersion in water for 1 minute, demonstrating their fast response to water. The interlayer distance of EGO membrane increased slightly from 1.12 nm to 1.17 nm after immersion in water for 1 hour, and remained constant at 1.18 nm for the testing period of 7 days. With regards to the CGO membrane, its interlayer distance progressively increased with increased immersion time from 1.27 nm (1 minute) to 1.40 nm (1 day). This behaviour is similar to previous reports where the interlayer distance of CGO membrane displayed a continuous increase to ~6 nm due to the intercalation of water molecules.[14] Due to the limitations of XRD technique, the CGO peak was not able to be detected after 1 day of immersion. The XRD pattern of EGO membranes immersed for 7 days (**Figure 2d**) can be fitted with two component peaks: GO-1 and GO-2, centred on about 9.1° and 7.6°, respectively, corresponding to interlayer distances of 0.92 nm and 1.16 nm, which represents one and two water monolayers between GO sheets. The majority part of peak comes from GO-2 peak, indicating a stable two-layer water molecule structure within EGO membrane after immersion for 7 days (For detailed discussion about structural change with immersion time of EGO and CGO membranes, see **ESI-3** and **Figure S7-S8**). This stable and consistent interlayer spacing of EGO represents an equilibrated state that is most likely determined by the interplay of attractive hydrogen bonding/sp^2 domains and repulsive negative ion charges (*e.g.* carboxylic acid).

GO membranes have been widely employed as promising separation membranes for nanofiltration and desalination.[28-30] Ionic sieving and water permeation properties of EGO membranes and CGO membranes were investigated. To measure the permeation of Na^+, a 0.1 M NaCl solution was used in the feed compartment. The amounts of Na^+ ions permeated through membranes with time were measured by monitoring the electrical conductivity change of permeate compartments.

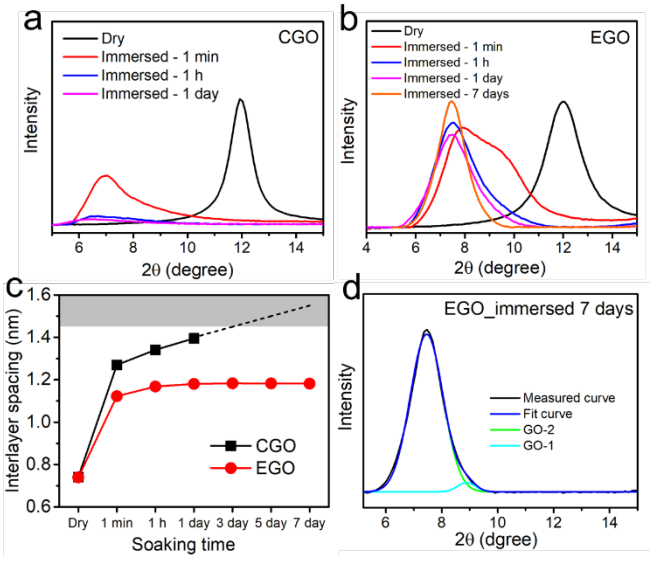

Figure 2 XRD patterns for (a) CGO membranes and (b) EGO membranes at different immersion times in water of neutral pH. (c) Interlayer spacing change with immersion time. The shaded grey area is beyond the detection limit. XRD patterns with fitting peaks: GO-1 (9.1°) and GO-2 (7.6°) for EGO membrane after immersion in neutral water for 7 days.

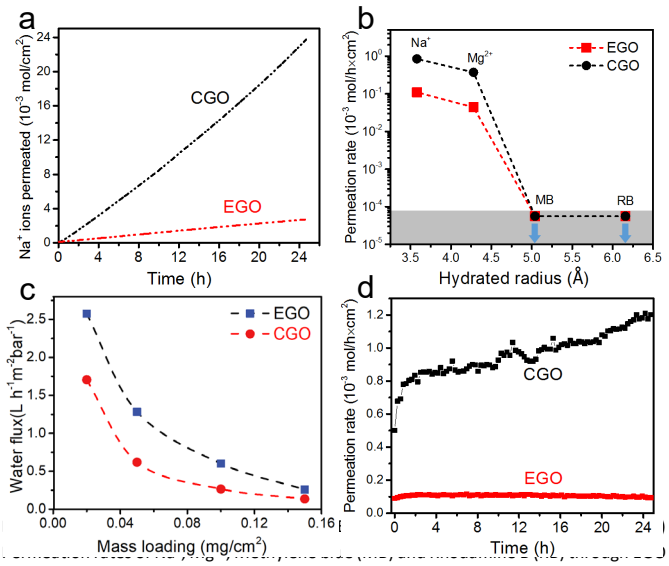

and CGO membranes. The grey area is below the detection limit. (c) Water flux through EGO and CGO membranes at different mass loadings. (d) Na^+ permeation rate change with permeation time.

It can be seen in **Figure 3a** that Na^+ ions concentration in permeate compartments increase with time for both EGO and CGO membranes. Specifically, EGO shows much reduced amounts of Na^+ ions permeating through the membrane, compared with CGO. In addition to the Na^+ ions permeation, the permeations rates of Mg^{2+}, MB and RB through the membranes were also tested, with the results shown in **Figure 3b**. Evidently, the permeation rate shows a significant decrease above a hydrated radius of about 4.5 Å, which is in good agreement with the previous research.[11] MB and RB molecules show extremely low permeation, and no permeation was detected for both EGO and CGO membranes. As for ions, the EGO membrane showed about 8 times lower permeation rates for Na^+ and Mg^{2+}, than observed in CGO membranes. Despite higher rejections for ions, the water flux of EGO membranes was not reduced. As shown in **Figure 3c**, the water flux of EGO membranes is even much higher than that of CGO membranes at different mass loadings. The stabilities of EGO and CGO membranes in the ionic sieving process were also examined by measuring the permeation rate of Na^+ with prolonged permeation for up to 24 hours, as shown in **Figure 3d**. The permeation rate of CGO membrane showed a significant increase over the first 3 hours, due to a strong increase of interlayer spacing when CGO membrane was swollen within the aqueous solution. It subsequently showed a more gradual increase during the next 21 hours, which is caused by a continuously increasing interlayer distance within the CGO membranes. In contrast, the ion permeation rate showed a slight increase in the first two hours and kept constant for at least 24 hours, demonstrating its stable structure in aqueous solution. Similarly, in pressure-driven filtration, EGO membranes also showed higher rejection for the ions and molecules while kept higher permeance (**ESI-4** and **Figure S9**), which further illustrates the better stability of EGO membranes than CGO membranes. Such combination makes EGO membranes a promising candidate to be used in water-based applications, such as ion sieving or desalination.

To understand the high stability and superior ionic sieving of EGO membranes, the structure and chemical groups of EGO have been characterized by Raman spectroscopy and X-ray photoelectron spectroscopy (XPS). The differences in structures and chemical groups of CGO and EGO can provide insights to their different stability in aqueous solution. **Figure 4a, b** show Raman spectra of EGO and CGO in the first-order region from 1000 cm^{-1} to 1900 cm^{-1} with fitted D peak, G peak and D'' peak. The main parameters of the peaks are displayed in **Table 1**. From Raman analysis (see more details in **ESI-5**), EGO exhibits much larger aromatic domain size (11.4 nm) than CGO (1.3 nm), which goes to show that EGO has a more ordered and crystalline structure. When the membrane is immersed in aqueous solutions, the interactions of the aromatic domains will assist the membranes to retain a more ordered structure, with a well-maintained interlayer distance. This balanced hydrophobic and hydrophilic interactions within the EGO membrane has contributed to its high stability in water and good ionic sieving properties. Moreover, the larger aromatic region of EGO can also explain its greater water flux according to the model proposed by Joshi et al[11] which proposed that water shows frictionless flow in the pristine graphene regions. In addition, EGO contains smaller percentage of carboxylic acid groups (3.5 %) than CGO (8.4 %) from XPS spectra shown in **Figure 4c, d** (see more details in **ESI-5**). It is well known that carboxylic acid groups can be easily ionized in aqueous solution, especially in alkaline solution, and can lead to electrostatic repulsive forces between graphene oxide sheets. This will cause an increase in the interlayer spacing between graphene oxide sheets, which leads to poor structural stability of laminated GO membranes. Hydroxyl groups, conversely, can form attractive hydrogen bonding between the sheets. Therefore, apart from the larger aromatic domains,

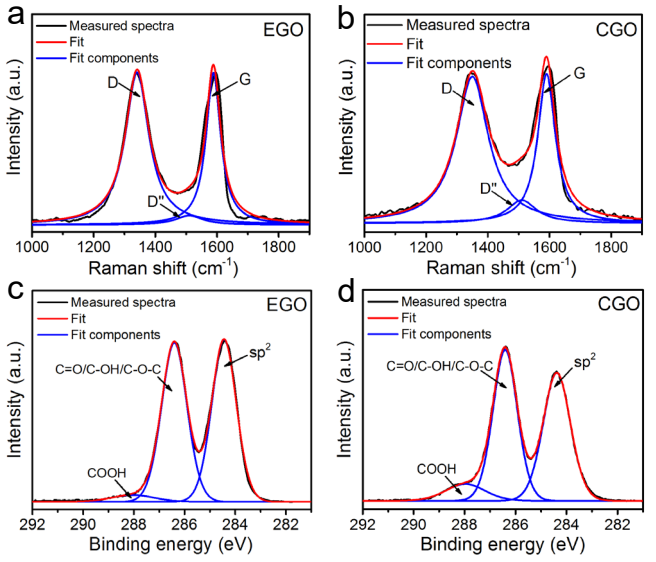

Figure 4 Raman spectrum of (a) EGO and (b) CGO in the first order region (1000 cm^{-1} – 1900 cm^{-1}). X-ray photoelectron (XPS) spectra of (c) EGO and (d) CGO in the C1s region (281 – 292 eV).

Table 1 Comparison of the main peak parameters in Raman spectra for CGO and EGO

	FWHM (cm-1)				
	D	G	ID/IG	La (nm)	ID''/IG
EGO	92.9	57.4	0.99	11.4	0.06
CGO	126.1	69.1	0.98	1.3	0.15

lower carboxylic acid and higher hydroxyl content of EGO also contribute to the membrane stability in water.

In conclusion, we fabricated crosslinker-free EGO membranes with unexpected structural stability in water. The interlayer distance between the hydrated EGO sheets was found to be very consistent (at 1.18 nm) after prolonged immersion in water or even being subjected to vigorous shaking. Furthermore, EGO membrane exhibited superior ionic sieving and water filtration performance than CGO membranes, with a much higher stability, ionic rejection and water flux. The high stability and good ionic sieving performance of EGO membranes are ascribed to the large aromatic domain size and low carboxylic acid content of EGO sheets. Given that GO-based membrane is being actively explored for a broad range of water treatment applications, the extraordinary stability of EGO membranes in aqueous solutions will be of great interest and significance to both the scientific and industrial communities.

Conflicts of interest

There are no conflicts to declare.

Notes and references

1. A. W. Mohammad, Y. H. Teow, W. L. Ang, Y. T. Chung, D. L. Oatley-Radcliffe and N. Hilal, *Desalination*, 2015, **356**, 226-254.
2. M. M. Pendergast and E. M. V. Hoek, *Energy & Environmental Science*, 2011, **4**, 1946-1971.
3. P. Marchetti, M. F. Jimenez Solomon, G. Szekely and A. G. Livingston, *Chemical Reviews*, 2014, **114**, 10735-10806.
4. R. K. Joshi, S. Alwarappan, M. Yoshimura, V. Sahajwalla and Y. Nishina, *Applied Materials Today*, 2015, **1**, 1-12.
5. G. Liu, W. Jin and N. Xu, *Chemical Society Reviews*, 2015, **44**, 5016-5030.
6. H. Huang, Y. Ying and X. Peng, *Journal of Materials Chemistry A*, 2014, **2**, 13772-13782.
7. H. W. Kim, H. W. Yoon, S.-M. Yoon, B. M. Yoo, B. K. Ahn, Y. H. Cho, H. J. Shin, H. Yang, U. Paik, S. Kwon, J.-Y. Choi and H. B. Park, *Science*, 2013, **342**, 91-95.
8. J. Shen, G. Liu, K. Huang, W. Jin, K.-R. Lee and N. Xu, *Angewandte Chemie*, 2015, **127**, 588-592.
9. R. R. Nair, H. A. Wu, P. N. Jayaram, I. V. Grigorieva and A. K. Geim, *Science*, 2012, **335**, 442-444.
10. K. Huang, G. Liu, Y. Lou, Z. Dong, J. Shen and W. Jin, *Angewandte Chemie International Edition*, 2014, **53**, 6929-6932.
11. R. K. Joshi, P. Carbone, F. C. Wang, V. G. Kravets, Y. Su, I. V. Grigorieva, H. A. Wu, A. K. Geim and R. R. Nair, *Science*, 2014, **343**, 752-754.
12. J. Abraham, K. S. Vasu, C. D. Williams, K. Gopinadhan, Y. Su, C. T. Cherian, J. Dix, E. Prestat, S. J. Haigh, I. V. Grigorieva, P. Carbone, A. K. Geim and R. R. Nair, *Nat Nano*, 2017, **advance online publication**.
13. L. Chen, G. Shi, J. Shen, B. Peng, B. Zhang, Y. Wang, F. Bian, J. Wang, D. Li, Z. Qian, G. Xu, G. Liu, J. Zeng, L. Zhang, Y. Yang, G. Zhou, M. Wu, W. Jin, J. Li and H. Fang, *Nature*, 2017, **advance online publication**.
14. S. Zheng, Q. Tu, J. J. Urban, S. Li and B. Mi, *ACS Nano*, 2017, **11**, 6440-6450.
15. C.-N. Yeh, K. Raidongia, J. Shao, Q.-H. Yang and J. Huang, *Nat Chem*, 2015, **7**, 166-170.
16. K. H. Thebo, X. Qian, Q. Zhang, L. Chen, H.-M. Cheng and W. Ren, *Nature Communications*, 2018, **9**, 1486.
17. X.-L. Xu, F.-W. Lin, Y. Du, X. Zhang, J. Wu and Z.-K. Xu, *ACS Applied Materials & Interfaces*, 2016, **8**, 12588-12593.
18. Y. T. Nam, J. Choi, K. M. Kang, D. W. Kim and H.-T. Jung, *ACS Applied Materials & Interfaces*, 2016, **8**, 27376-27382.
19. H. Liu, H. Wang and X. Zhang, *Advanced Materials*, 2015, **27**, 249-254.
20. Y. Han, Z. Xu and C. Gao, *Advanced Functional Materials*, 2013, **23**, 3693-3700.
21. P. Yu, Z. Tian, S. E. Lowe, J. Song, Z. Ma, X. Wang, Z. J. Han, Q. Bao, G. P. Simon, D. Li and Y. L. Zhong, *Chemistry of Materials*, 2016, **28**, 8429-8438.
22. Z. Tian, P. Yu, S. E. Lowe, A. G. Pandolfo, T. R. Gengenbach, K. M. Nairn, J. Song, X. Wang, Y. L. Zhong and D. Li, *Carbon*, 2017, **112**, 185-191.
23. S. Pei, Q. Wei, K. Huang, H.-M. Cheng and W. Ren, *Nature Communications*, 2018, **9**, 145.
24. P. Yu, S. E. Lowe, G. P. Simon and Y. L. Zhong, *Current Opinion in Colloid & Interface Science*, 2015, **20**, 329-338.
25. S. Yang, M. R. Lohe, K. Müllen and X. Feng, *Advanced Materials*, 2016, **28**, 6213-6221.
26. H. Chen, C. Li and L. Qu, *Carbon*, 2018, **140**, 41-56.
27. J. Cao, P. He, M. A. Mohammed, X. Zhao, R. J. Young, B. Derby, I. A. Kinloch and R. A. W. Dryfe, *Journal of the American Chemical Society*, 2017, **139**, 17446-17456.
28. H. Huang, Z. Song, N. Wei, L. Shi, Y. Mao, Y. Ying, L. Sun, Z. Xu and X. Peng, *Nature Communications*, 2013, **4**, 2979.
29. A. Morelos-Gomez, R. Cruz-Silva, H. Muramatsu, J. Ortiz-Medina, T. Araki, T. Fukuyo, S. Tejima, K. Takeuchi, T. Hayashi, M. Terrones and M. Endo, *Nat Nano*, 2017, **advance online publication**.
30. A. Akbari, P. Sheath, S. T. Martin, D. B. Shinde, M. Shaibani, P. C. Banerjee, R. Tkacz, D. Bhattacharyya and M. Majumder, *Nature Communications*, 2016, **7**, 10891.